Journal of Materials Chemistry A

COMMUNICATION

View Article Online
View Journal

Cite this: DOI: 10.1039/c4ta02583k

Received 23rd May 2014
Accepted 4th July 2014

DOI: 10.1039/c4ta02583k

www.rsc.org/MaterialsA

In situ environmental transmission electron microscopy study of oxidation of two-dimensional Ti_3C_2 and formation of carbon-supported TiO_2†

H. Ghassemi, W. Harlow, O. Mashtalir, M. Beidaghi, M. R. Lukatskaya, Y. Gogotsi and M. L. Taheri*

Two-dimensional Ti_3C_2, also known as "MXene", was oxidized in air under two different oxidizing regimes in order to produce carbon-supported TiO_2. *In situ* TEM analysis coupled with Raman spectroscopy revealed the formation of either anatase nanoparticles or planar rutile nanocrystals, which were controlled by the time, temperature and heating rate.

Titanium dioxide (TiO_2) is an excellent candidate for photocatalysis[1–3] and energy generation and storage[4–6] applications, due to its 3.2 eV band gap. Additionally, its non-toxicity and thermal and chemical stability enable various other applications for self-cleaning and purification purposes.[7] Nevertheless, applications of pure TiO_2 are limited due to its relatively wide band gap with a narrow wavelength response range and rapid recombination of photoinduced electron–hole pairs, or, as in the case of energy storage related applications, due to moderate values of the storage capacity as well as low conductivity. Over decades, researchers have been working on designing new TiO_2-based systems in order to overcome those limitations. Combining TiO_2 with carbon and carbon-based materials is a promising route to enhance its photocatalytic activity and other properties by facilitating the transport of electrons through carbon, which reduces the recombination effect, and increasing the accessible surface area of TiO_2.[8] Some of the most common methods of synthesis of TiO_2 supported on carbonaceous nanomaterials include the sol–gel technique[9] and chemical vapour deposition.[10] In the sol–gel method, tetrabutyl titanate and graphite oxide are commonly used as precursors and composites of TiO_2 (anatase) and graphene sheets can be obtained upon reactions of hydrolysis and polycondensation.[11,12]

Recently, flash oxidation of 2D Ti_3C_2, a representative of a large family of novel two-dimensional (2D) ternary metal carbides and carbonitrides named MXenes,[13,14] was proposed as an alternative one-step synthesis method, which can provide the well-controlled formation of TiO_2 on carbon.[15] The starting material was produced by selective extraction of the Al atoms from Ti_3AlC_2 through treatment in hydrofluoric acid.[13] It can be delaminated into single- or few-layer flakes by intercalation with dimethyl sulfoxide followed by sonication in water. Along with metallic in-plane conductivity, the MXene has a hydrophilic surface, terminated with functional groups, such as –OH, –F and –O–, and its chemical formula is referred to as $Ti_3C_2T_x$, where T stands for the "terminating group" and x is the number of surface groups per Ti_3C_2 unit cell. It was shown that $Ti_3C_2T_x$ has good Li-ion capacity and high volumetric capacitance in aqueous electrolytes.[16] Based on previous studies of the oxidation behavior of bulk TiC[17–19] in various temperature ranges, and under various oxygen partial pressures, it is known that the final product is TiO_2 and its morphology can be tuned by changing the oxidation conditions. Recently, it was shown that treatment of layered $Ti_3C_2T_x$ at elevated temperatures in air or flowing CO_2 results in the formation of anatase TiO_2 embedded in amorphous carbon sheets; however, the mechanisms by which the oxidation of MXene and the formation of intermediate TiO_2 phases occurred were unknown.[15] *In situ* transmission electron microscopy (TEM) techniques can shed light on oxidation behavior of $Ti_3C_2T_x$.

This work presents insights into the mechanism of transformation of $Ti_3C_2T_x$ into the TiO_2/carbon hybrid material during oxidation in air at different temperatures and under different heating rates. We conducted oxidation of $Ti_3C_2T_x$ inside a TEM column and showed the controllable formation of anatase and rutile polymorphs using *in situ* environmental TEM coupled with Raman spectroscopy.

Using a Protochips™ environmental stage inside a TEM (JEOL JEM-2100, Japan), we explored two oxidation regimes – flash oxidation and slow heating – with different heating ranges and rates, as well as environmental exposure times. During heating in the presence of an oxidizing environment, diffraction patterns were taken simultaneously with TEM bright field

Department of Materials Science and Engineering, A.J. Drexel Nanomaterials Institute, Drexel University, Philadelphia, PA 19104, USA. E-mail: mtaheri@coe.drexel.edu

† Electronic supplementary information (ESI) available: SEM-EDS of the final products for each oxidizing regimes. See DOI: 10.1039/c4ta02583k

imaging. To confirm the formation of TiO_2 phases, Raman spectroscopy was performed on oxidized samples using a Raman spectrometer (Renishaw inVia, Gluocestershire, UK) with an argon ion laser (514.5 nm) focused to a spot size of ~2 μm with a power of less than 1 mW.

For each *in situ* TEM experiment, a droplet of aqueous colloidal solution of delaminated $Ti_3C_2T_x$ flakes was dried on the environmental cell's heating chip platform. After drying in air at room temperature, the cells were sealed in ambient air. The two different oxidation regimes used in this study are shown in Fig. 1. Flash oxidation was carried out by increasing the temperature stepwise to 950 °C, in order to keep the image in focus due to bending of the heating chip, and then kept at that temperature for ~1 min in air to mimic furnace oxidation experiments.[15] To analyse the slow oxidation regime, pristine sheets were heated up to 450 °C at a rate of 0.1 °C s^{-1} and kept at this temperature for ~2 h to characterize possible phase transformation.

The evolution of the particles during stepwise increase of temperature is shown in Fig. 2a–d. Fig. 2d–i show snapshots of this experiment at 950 °C where the Ti layers initially breakdown into large pieces/islands, as indicated with white arrows. Black arrows indicate the same particle in each snapshot for drift compensation. These large, distinct particles could be clearly seen just four seconds after the breakdown of Ti layers and were observed to shrink in diameter, as indicated in Fig. 2f. Based on the observed shrinkage in the lateral size of particles, plotted in Fig. 2l, and image contrast changes, it can be concluded that these particles are first formed in a planar thin film morphology and subsequently shrink laterally and grow vertically into 3D particles *via* inter-layer diffusion and by consuming the smaller particles by Ostwald ripening.[20] After 66 s of flash oxidation (total of 88 s), the sample was cooled to room temperature, and the low-magnification and high-resolution TEM images revealed a relatively uniform dispersion of

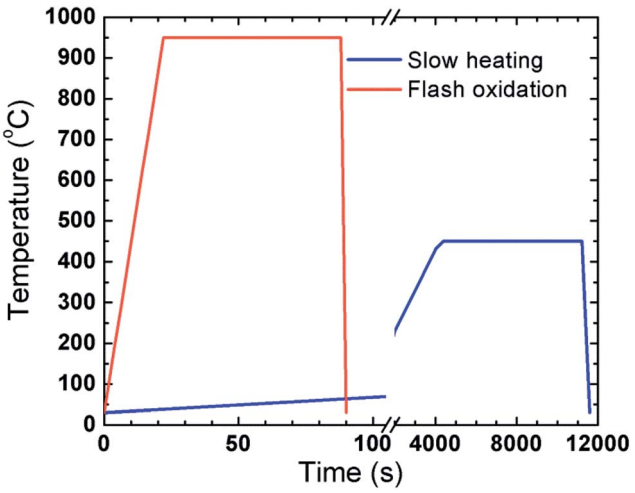

Fig. 1 Two oxidation regimes. Flash oxidation was performed by rapidly heating the sample to 950 °C and keeping it at this temperature for ~1 min. Slow heating was carried out by heating the sample to 450 °C at 0.1 °C s^{-1} rate and keeping it at this temperature for ~2 h.

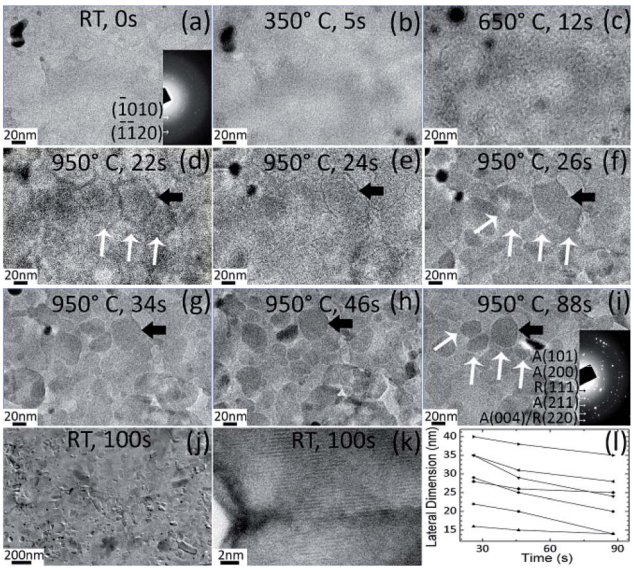

Fig. 2 TEM snapshots of the flash oxidation of $Ti_3C_2T_x$. (a) represents the TEM image of the pristine sample at room temperature. (b–d) show stepwise increase in the temperature up to 950 °C within 22 s leading to the formation of grains in (d). (e–i) represent formation and lateral shrinking/coarsening of TiO_2 particles. (j–k) represent low magnification and HRTEM images of the sample after cooling back to room temperature. Insets in (a) and (i) show plot of lateral dimension shrinking as a function of time for several different nanoparticles. Black dots are Au nanoparticles that served as an internal standard for lattice fringe and diffraction studies.

TiO_2 particles (Fig. 2j and k). A lattice spacing of 3.8–3.9 Å was measured from HRTEM images, which corresponds to (101) planes in anatase (JCPDS #71–1167). Selected area electron diffraction (SAD) patterns before and after flash oxidation (see insets in Fig. 2a and i, respectively) confirmed formation of mainly the anatase phase while two rings overlap with those of the rutile phase. For the slow oxidation regime, the formation of oxide particles is illustrated in Fig. 3a–f. Fig. 3a shows the top view of the pristine $Ti_3C_2T_x$ sheet with the corresponding diffraction pattern in the inset. As shown in Fig. 3b–d, upon slowly increasing the temperature, the Ti layers transformed into a granular structure. Simultaneous diffraction patterns indicated the formation of mainly a rutile structure while two rings overlapped with those of the anatase phase. HRTEM imaging revealed a nanocrystalline structure with a lattice spacing of 4.4 Å corresponding to (110) for both electron-beam irradiated and non-irradiated portions of the sample (JCPDS #88–1175), shown in Fig. 3e and f, respectively. Therefore, the effect of electron beam on the phase transition can be negated. Moreover, the beam effect can be addressed by the fact since MXene flakes are thermally conductive, heating due to electron beam is negligible. Regarding knock-on and sputtering damage under the electron beam, it has been shown that the transferable energy at 200 keV is much less than Ti displacement threshold and also no visible damage was observed while imaging the pristine sample.[21,22]

Raman spectroscopy of the flash oxidized sample, Fig. 4a, confirmed the formation of mainly the anatase TiO_2 phase and

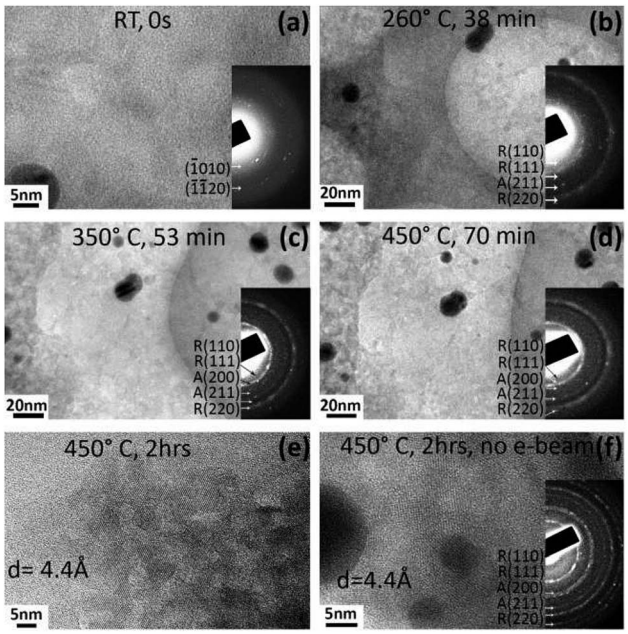

Fig. 3 TEM snapshots of slow oxidation of $Ti_3C_2T_x$. (a) represents the pristine sample at room temperature. (b–d) show a step-wise increase of the temperature up to 450 °C and insets are the corresponding SADs at indicated temperatures. (e) shows the HRTEM image of the nanocrystalline structure, after 2 h at 450 °C. (f) shows a bright-field TEM image and an SAD pattern of another region of the same sample at 450 °C, which was not irradiated with an electron beam.

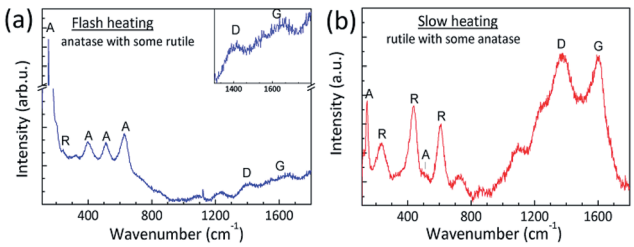

Fig. 4 (a) Raman spectra showing the final stage of oxidation and confirming the formation of the anatase structure with traces of rutile. (b) shows the formation of rutile nanocrystals as well as some anatase.

traces of the rutile phase was also found, in agreement with the SAD indexing shown in Fig. 2. The slow heating led to formation of mainly rutile, with traces of the anatase phase (Fig. 4b). Scanning electron microscopy (SEM) combined with energy dispersive X-ray analysis (see ESI Fig. S1 and Table S1†) of samples oxidized using both regimes revealed an excess of oxygen compared to that of the pristine sample, which further supported the idea of oxidation of Ti layers. Peaks at ~1400 cm^{-1} and 1600 cm^{-1} correspond to D and G bands in carbon, which represent disordered and graphitic structures, respectively. These two bands are clearly pronounced in the case of slow heating since there is enough time for carbon to reorganize, while in the case of the flash oxidation regime, due to short duration of the process, carbon is disordered and the Raman peak intensities are lower. One can expect oxidation of carbon to occur simultaneously with the formation of TiO_2; however, the Gibbs energy for Ti oxidation is more negative than that of the carbon, which results in preferred oxidation of Ti.[23] Formation of free carbon under the TiO_2 layer was observed upon oxidation of TiC ceramics.[17] Nevertheless, the oxidation of carbon can take place after the Ti layers are all oxidized. Hence, in the slow heating regime, since there is enough time and an ample source of oxygen, the carbon concentration is lower (ESI Table S1†) than that of the pristine and flash oxidized samples.

In Fig. 5, a schematic illustration represents the transformation of MXene flakes into anatase or rutile structures as observed during the *in situ* TEM experiments. We assume that during the flash oxidation and upon diffusion of oxygen, homogeneous nucleation of anatase nanoparticles takes place on the top and bottom Ti layers (Fig. 5b), where Ti atoms are directly exposed to oxygen. 2D nuclei grow vertically into 3-D nanoparticles, while shrinking in lateral dimensions. Lateral shrinkage of these nanoparticles is accompanied by diffusion of Ti atoms from the middle layer to the MXene flake surfaces. This is due to the fact that the distance a Ti atom has to travel from the middle layer becomes shorter than those on the top and bottom layers. Therefore, completion of oxidation of MXene flakes results in formation of anatase nanoparticles supported by carbon sheets, Fig. 5c. Similarly, during slow oxidation (illustrated schematically in Fig. 5d), it is assumed that the entire top and bottom Ti layers first transform into sheets of nanocrystalline rutile. Therefore, since the nucleation is not site-specific and takes place throughout the entire layers, it can be considered homogeneous. It is then followed by diffusion of Ti from the middle layer toward the source of oxygen. Note that the diffraction patterns of samples from both oxidation regimes correspond to TiO_2 phases and do not show presence of any Ti metal or cubic TiC. Note that *ex situ* flash oxidation of MXene flakes inside a furnace at comparable temperatures also confirmed formation of carbon-supported anatase nanoparticles *via* TEM, SEM and Raman analysis.[15] It should be noted that oxidation of Ti is expected to start with formation of small particles of anatase, followed by coarsening and transforming into rutile particles, from the thermodynamic

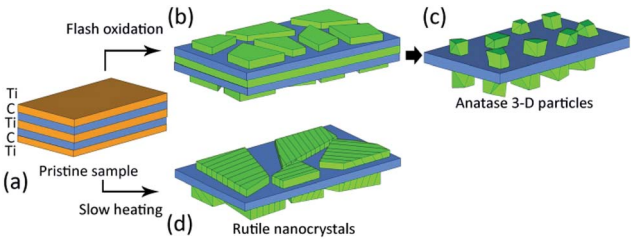

Fig. 5 Schematic of the oxidation mechanisms under two oxidation regimes. (a) shows the pristine layered structure of MXene. (b) and (c) represent the flash oxidation mechanism, where the top and bottom Ti layers are first oxidized to form very thin anatase nanoparticles, followed by diffusion of Ti from the middle layer to complete growth of 3D nanoparticles. (d) shows a slow oxidation mechanism, when the top and bottom Ti layers oxidize first, followed by diffusion of Ti from the middle layer into the oxide film.

viewpoint. However, our results showed formation of rutile sheets directly from the pristine Ti phase, without formation of an intermediate anatase phase.

By manipulating the temperature, heating rate and oxidation time, one can control the phase composition and morphology of TiO_2. Oxidation at higher temperatures for a short period of time (flash oxidation) results in the formation of primarily anatase nanoparticles, whereas slow heating over an extended period of time at lower temperatures leads to the formation of thin sheets of rutile. It is important to note that since partial oxidation of carbon in our samples is possible, further investigation is required to quantify the final carbon/TiO_2 ratio. Also, a different MXene, Ti_2C,[14] can be used instead of Ti_3C_2 to control the carbon/TiO_2 ratio in the product.

Compared to common multi-step methods for deposition of oxides on carbon materials, the method we describe herein is a single-step treatment, which results in controlled formation of TiO_2 on amorphous 2D carbon sheets. Since about ten MXenes have been reported[14,24] and many more are expected to be produced soon, other carbon–metal oxide hybrids can be synthesized using the described approach.

Conclusions

We have demonstrated that under oxidizing environments, 2D $Ti_3C_2T_x$ MXene can be converted into carbon sheet-supported TiO_2 of different crystal structures, particle sizes and morphologies. The oxidation process can be predictively controlled by the heating rate, temperature range, and exposure time. Anatase nanoparticles are obtained *via* flash oxidation, while rutile sheets form during slow heating. These results support the possibility of producing different nanoparticle assemblies by using precursors with desired morphologies and composition, which eliminates several synthesis steps, and is faster and better controlled compared to the existing methods.

Acknowledgements

This research was supported by the National Science Foundation grant # 1031403 and Department of Energy NEUP contract # CFP-11-2215. The work of Y.G. and M.B. was supported by the Fluid Interface Reactions, Structures and Transport (FIRST) Center, an Energy Frontier Research Center funded by the U.S. Department of Energy, Office of Science, Office of Basic Energy Sciences. The authors are thankful to Michael Naguib and Michel W. Barsoum for support and useful discussions, Chang E. Ren for providing samples of delaminated $Ti_3C_2T_x$ for *in situ* TEM study, and the Centralized Research Facility of Drexel University for use of TEM and SEM.

References

1 A. Fujishima, Electrochemical Photolysis of Water at a Semiconductor Electrode, *Nature*, 1972, **238**(5358), 2.
2 H. Zhang, G. Chen and D. W. Bahnemann, Photoelectrocatalytic materials for environmental applications, *J. Mater. Chem.*, 2009, **19**(29), 5089–5121.
3 Z. Lai, *et al.*, A new insight into regulating high energy facets of rutile TiO_2, *J. Mater. Chem. A*, 2013, **1**(13), 4182–4185.
4 Z. Hong and M. Wei, Layered titanate nanostructures and their derivatives as negative electrode materials for lithium-ion batteries, *J. Mater. Chem. A*, 2013, **1**(14), 4403–4414.
5 M. Gratzel, Photoelectrochemical cells, *Nature*, 2001, **414**(6861), 7.
6 J. S. Chen, *et al.*, Carbon-supported ultra-thin anatase TiO_2 nanosheets for fast reversible lithium storage, *J. Mater. Chem.*, 2011, **21**(15), 5687–5692.
7 A. Fujishima, X. Zhang and D. A. Tryk, TiO_2 photocatalysis and related surface phenomena, *Surf. Sci. Rep.*, 2008, **63**(12), 515–582.
8 R. Leary and A. Westwood, Carbonaceous nanomaterials for the enhancement of TiO_2 photocatalysis, *Carbon*, 2011, **49**(3), 741–772.
9 U. G. Akpan and B. H. Hameed, The advancements in sol–gel method of doped-TiO_2 photocatalysts, *Appl. Catal., A*, 2010, **375**(1), 1–11.
10 G. Li Puma, *et al.*, Preparation of titanium dioxide photocatalyst loaded onto activated carbon support using chemical vapor deposition: A review paper, *J. Hazard. Mater.*, 2008, **157**(2–3), 209–219.
11 X.-Y. Zhang, *et al.*, Graphene/TiO_2 nanocomposites: synthesis, characterization and application in hydrogen evolution from water photocatalytic splitting, *J. Mater. Chem.*, 2010, **20**(14), 2801–2806.
12 Y. Liang, *et al.*, TiO_2 nanocrystals grown on graphene as advanced photocatalytic hybrid materials, *Nano Res.*, 2010, **3**(10), 701–705.
13 M. Naguib, *et al.*, Two-Dimensional Nanocrystals Produced by Exfoliation of Ti_3AlC_2, *Adv. Mater.*, 2011, **23**(37), 4248–4253.
14 M. Naguib, *et al.*, Two-dimensional transition metal carbides, *ACS Nano*, 2012, **6**(2), 1322–1331.
15 M. Naguib, *et al.*, One-step synthesis of nanocrystalline transition metal oxides on thin sheets of disordered graphitic carbon by oxidation of MXenes, *Chem. Commun.*, 2014, **50**(56), 7420–7423.
16 M. R. Lukatskaya, *et al.*, Cation Intercalation and High Volumetric Capacitance of Two-Dimensional Titanium Carbide, *Science*, 2013, **341**(6153), 1502–1505.
17 S. Shimada and M. Kozeki, Oxidation of TiC at low temperatures, *J. Mater. Sci.*, 1992, **27**(7), 1869–1875.
18 A. Onuma, *et al.*, High temperature oxidation of sintered TiC in an H_2O-containing atmosphere, *Solid State Ionics*, 2004, **172**(1–4), 417–419.
19 Y. G. Gogotsi and V. A. Lavrenko, *Corrosion of High-performance Ceramics*, Springer, Berlin, 1992.
20 W. Ostwald, Über die vermeintliche Isomerie des roten und gelben Quecksilberoxyds und die Oberflächenspannung fester Körper, *Z. Phys. Chem.*, 1900, **13**, 9.

21 R. F. Egerton, P. Li and M. Malac, Radiation damage in the TEM and SEM, *Micron*, 2004, **35**(6), 399–409.
22 D. B. Williams and C. B. Carter, The Transmission Electron Microscope, in *Transmission Electron Microscopy*, Springer, 2009, pp. 3–22.
23 Y. Qin, *et al.*, Oxidation of *in situ* synthesized TiC particle-reinforced titanium matrix composites, *Mater. Sci. Eng., A*, 2005, **404**(1–2), 42–48.
24 M. Naguib, *et al.*, MXenes: A New Family of Two-Dimensional Materials, *Adv. Mater.*, 2014, **26**(7), 992–1005.